New Constraints on Companions and Dust within a few AU of Vega

B. Mennesson[1], E. Serabyn[1], C. Hanot[2], S. R. Martin[1], K. Liewer[1], D. Mawet[1]

bertrand.mennesson@jpl.nasa.gov

ABSTRACT

We report on high contrast near infrared ($\sim 2.2~\mu$m) observations of Vega obtained with the Palomar Fiber Nuller, a dual sub-aperture rotating coronagraph installed at the Palomar Hale telescope. Our data show consistent astrophysical null depth measurements at the $\simeq 10^{-3}$ level or below for three different baseline orientations spanning 60 degrees in azimuth, with individual 1 σ uncertainties $\leq 7 \times 10^{-4}$. These high cancellation and accuracy levels translate into a dynamic range greater than 1000:1 inside the diffraction limit of the 5 m telescope beam. Such high contrast performance is unprecedented in the near infrared, and provides improved constraints on Vega's immediate ($\simeq 20$ to 250 mas, or $\simeq 0.15$ to 2 AU) environment. In particular, our measurements rule out any potential companion in the [0.25 - 1AU] region contributing more than 1% of the overall near infrared stellar flux, with limits as low as 0.2% near 0.6 AU. These are the best upper limits established so far by direct imaging for a companion to Vega in this inner region. We also conclude that any dust population contributing a significant ($\geq 1\%$) near infrared *thermal* excess can arise only within 0.2 AU of the star, and that it must consist of much smaller grains than in the solar zodiacal cloud. Dust emission from further than $\simeq 2$ AU is also not ruled out by our observations, but would have to originate in strong scattering, pointing again to very small grains.

Subject headings: infrared: stars — instrumentation: coronagraphs — stars: circumstellar matter — stars: individual (Vega)

[1]Jet Propulsion Laboratory, California Institute of Technology, 4800 Oak Grove Drive, Pasadena CA 91109-8099

[2]AEOS, University of Liège, Allée du 6 Août, 17 Bât B5c, 4000 Liège, Belgium

1. Introduction

Planets are believed to form out of the material in circumstellar disks known to exist around young stars. The pre-planetary disks are generally quite bright, and have been very well studied at high angular resolution by interferometry in recent years (e.g. Monnier et al. 2005; Millan-Gabet et al. 2006; Tannirkulam et al. 2008). As planets are formed, the opacity of the primordial disk rapidly decreases, and a transition is observed to the regime of debris disks, with inner warmer regions commonly referred to as "exo-zodiacal clouds". Because zodiacal dust grain lifetimes are much shorter than stellar lifetimes, it is believed that zodiacal dust must be regenerated (Backman & Paresce 1993) to be present around main sequence stars. The inner (0.1 to 10 AU) distribution of exozodiacal dust in debris disks thus reflects dynamical interactions at the heart of planet formation, and so are of great scientific interest. More generally, the determination of the exo-zodiacal emission level and its central (< 10AU) spatial distribution around nearby main sequence stars has been long identified (e.g. Beichman & Velusamy 1997; Mennesson & Mariotti 1997) as crucial information, both for planetary formation and planet- disk interaction models, and for the design of direct exoplanet imaging space missions.

However, exo-zodiacal disks are generally much fainter and difficult to observe than proto-planetary disks. Debris disks observed to date around nearby stars (e.g. Holland et al. 1998; Siegler et al. 2007) are located predominantly far from their host stars (tens to hundreds of AU), and so are more analogous to our solar system's dusty Kuiper belt, located beyond our planetary belt, than to the $\sim$ AU-scale zodiacal disk inside our solar system's asteroid belt. This observational bias results from several factors: (i) small potential exozodiacal disk sizes, (ii) faintness relative to the host stars, and (iii) the use of long (far-infrared) observing wavelengths more sensitive to very cool dust. Detection of faint exozodiacal emission very near bright stars thus requires high angular resolution, and either a means of suppressing starlight or a high dynamic range. Near and mid-infrared high-resolution high-contrast interferometric instruments such as Fiber Linked Unit for Optical Recombination (FLUOR) on the CHARA array (Absil et al. 2006), the Bracewell Infrared Nulling Camera (BLINC) at the MMT (Liu et al. 2004) and the Keck Interferometer Nuller (KIN) (Colavita et al. 2009) have all tackled this issue of zodiacal light characterization. In both wavelength ranges, similar contrast levels were obtained in the inner 10 AU region of nearby main sequence stars: typically 0.2% at 1 σ. Quite surprisingly, this common instrumental performance has so far yielded many more excess detections in the near infrared than in the mid-infrared. Indeed, most mid-infrared results so far are upper limits: out of 23 nearby main sequence stars with no previously known far-infrared excess surveyed by one of the two main KIN key science programs, only one of them shows clear mid-infrared excess at the current detection levels (Millan-Gabet et al. 2011, in preparation). Con-

versely, in spite of the higher contrast expected, a larger fraction ($\simeq 20\%$, O. Absil and D. Defrère, private communication) of main sequence stars have shown significant (1%) near infrared excesses in their inner 10 AUs (Absil et al. 2006; Absil et al. 2008; Absil et al. 2009; Akeson et al. 2009; Di Folco et al. 2007). More detections of this kind are currently being unearthed by an on-going FLUOR survey. Interestingly, these same stars were surveyed in the mid-infrared with BLINC and KIN, and no excess was detected so far at current thresholds, except in the case of β Leo (Stock et al. 2010). These results have been interpreted as implying the presence of hot (≥ 500K) dust populations around a significant fraction of A to G main sequence stars - although the survey of a larger sample is required to derive robust statistics. Importantly, these putative bright exozodiacal disks appear much hotter than the zodiacal cloud, making the near infrared an optimal region for characterization of such hot dust. This also suggests that debris disk characteristics may strongly differ from our own zodiacal cloud, and that high contrast, near infrared interferometric observations might be a very powerful tool for conducting a statistical survey of exo-zodiacal disks.

In this context, a near infrared high dynamic range (10^{-4} to 10^{-3}) interferometric capability could provide an ideal solution for conducting deep surveys of exo-zodi clouds around nearby stars. It was one of the major drivers for the development of the fiber nulling approach (Haguenauer & Serabyn 2006; Serabyn & Mennesson 2006a; Mennesson et al. 2006) and the deployment of the Palomar Fiber Nuller (PFN) at the 5m̊ Hale telescope (Martin et al. 2008; Mennesson et al. 2010; Serabyn et al. 2010). High contrast observations with this technique promise to further our understanding of the hot dust phenomenon, whose actual origin remains unclear. Indeed, this excess could theoretically arise from thermal emission from hot dust - extended or restricted to annular inner regions-, more point-like structures such as clumps (perhaps resonant clumps), low mass companions, or even hot planetary embryos similar to those inferred around PMS stars such as AB Aur (Millan-Gabet et al. 2006), SR 21 (Eisner et al. 2009), and FU Ori (Malbet et al. 2005).

Since larger-scale debris disks detected in the FIR show a statistical dimming with stellar age (e.g. Siegler et al. 2007), the search for smaller-scale exozodiacal emission is likely best begun around fairly young, nearby stars with other evidence of dust. A prime candidate is therefore Vega, a nearby (7.8 pc) bright (0 mag) A0V star, with one of the first detections of excess FIR emission from a large debris disk (Aumann et al. 1985). Many of Vega's properties are well characterized, including its nearly pole-on orientation, its pole-to-equator temperature variation and limb darkening (Aufdenberg et al. 2006), and its nearly face-on large-scale debris disk (Wilner et al. 2002; Su et al. 2005). Moreover, some data regarding potential exozodiacal dust around Vega also exist: MIR limits on excess emission of $\simeq 2\%$ derived by MMT/BLINC (Liu et al. 2004; Liu et al. 2009) and by KI nulling (unpublished results), and a small near-infrared (NIR) short-baseline visibility deficit (Absil et al. 2006)

suggesting the presence of some very hot dust. Vega is thus perhaps an ideal first candidate for observations with the Palomar Fiber Nuller (PFN).

2. PFN Vega Observations and Results

Full descriptions of the PFN coronagraph hardware, observing procedure, and data reduction strategies are given in recent papers (Martin et al. 2008; Mennesson et al. 2010; Serabyn et al. 2010; Hanot et al. 2011). Vega was observed with the PFN in July 2009 with a constant 3.40 m baseline and three different azimuthal orientations spanning a range of 60 degrees. At each orientation, a four minute long sequence of null depth measurements was recorded. A statistical analysis of the measured fluctuating null depth distribution (Figure 1) is used to recover the underlying astrophysical null depth N_a, which is directly related to the source visibility [1]. More precisely, the astrophysical null depth is derived by minimizing a goodness of fit χ^2 test comparing the observed null distribution to a model distribution. Complete details about this "Null Self Calibration" method are given in Hanot et al. 2011. The error bar (1σ confidence interval) on N_a is first obtained by variation around its optimal value, using regular χ^2 statistics. However, this error bar estimation is only valid if the noise is dominated by a zero mean gaussian process. We then also conducted a bootstrapping analysis -independent of the actual noise properties -, resampling and replacing the observed null values, and generating many (500) fake null sequences derived from the observed data. Analyzing the corresponding sequences yields astrophysical null 1σ (68.3% confidence interval) uncertainties very similar to those derived using the χ^2 approach. The final error bar quoted on N_a is the largest of the uncertainties derived by the χ^2 and by the bootstrapping methods.

Table 1 summarizes Vega's astrophysical null depths derived as a function of baseline azimuth angle. All measured nulls have 1σ error bars smaller than 0.001. The orientation averaged null depth estimate, taking measurements scattering and individual uncertainties into account, is N_a= 0.0008 $\pm$ 0.0004 (weighted mean and weighted standard deviation). In comparison, adopting Vega's latest gravity darkened photospheric model (Aufdenberg et al. 2006), the expected null depth is 0.0004 at 2.2μm at the PFN 3.40 m baseline. (In fact Vega's photosphere is hardly resolved at this spatial resolution, and a more crude uniform disk model provides the same value at the 10^{-5} level). The residual null obtained after subtracting the 0.0004 diameter limited null depth characterizes a potential "excess leakage" above the photosphere. Its orientation average is then 0.0004 $\pm$ 0.0004, showing that the

---

[1]The astrophysical null depth is given by $N_a = \frac{(1-|V|)}{(1+|V|)}$, where V is the object's complex visibility

PFN observations do not detect any emission above that predicted for the photosphere that is statistically significant.

For each baseline orientation, Table 1 indicates the residual null measured on Vega (i.e the excess leakage obtained after subtraction of the photospheric null) and its 3σ upper limit. In order to convert the measured excess leakage to a true astrophysical excess, one must correct for the nuller sky transmission pattern, which is limited to about $300\,\mathrm{mas}$ FWHM (Mennesson et al. 2010). The maximum (3σ) relative flux compatible with the data is then derived at each of the 3 baseline orientations. At any given location in Vega's immediate environment (within $\simeq 2.3$ AU in radius), only the lowest of these 3 limits is retained. This yields the final "upper flux limit map" (Figure 3 left), i.e. the maximum (relative) K band flux of a companion as a function of its location. At the very center of the field, within 0.05 AU of Vega, the contribution of any off-axis source would be nulled out, and so no useful flux constraint can be derived. Similarly, our data do not reflect emission from sources located much further than $\simeq 3$AU, i.e. beyond the single-mode fiber field of view. Our data are most sensitive to the central [0.25 - 1 AU] region where we can rule out the presence of any companion contributing more than 1% of the overall K-band flux. This corresponds to the best point source upper limits derived so far by direct detection in this range of separations around Vega. At a given distance from Vega, the derived companion flux limit is a function of azimuth, reflecting the observed slight azimuthal variations as well as our incomplete (60°) span) baseline rotation. Figure 3 (upper right) shows as an example the upper limits derived at 0.6 AU as a function of azimuth angle, with values ranging from 0.2% to 0.6%. The residual "spikes" visible at azimuths of $\simeq 30$ and $\simeq 210$ degrees are expected, as these angles are 90 degrees away from the mean baseline orientation (117 degrees).

Potential stellar mass companions have already largely been ruled out within 10 AU of Vega by astrometric and radial velocity limits (Absil et al. 2006). But unlike gravitational techniques, our direct detection measurements can also impose strong constraints on the existence of extended sources of dust in the inner 1AU, e.g. on the relative contribution and physical characteristics of any putative hot debris disk around Vega. As there is strong evidence (Peterson et al. 1999; Aufdenberg et al. 2006) that Vega is viewed very nearly pole-on (inclination of $\sim 5°$), here we only consider circularly symmetric disk structures. As a convenient case to study, we further concentrate hereafter on geometrically thin (0.01AU) circular rings located at various radii.

As can be seen in Figure 3 (bottom right), the relative flux of a circular dust ring is best constrained by our data between 0.2 AU ($\simeq 25\,\mathrm{mas}$) and 1.1 AU ($\simeq 140$mas). In particular, we find that the existence of a geometrically thin ring contributing more than 0.6% of Vega's K band flux is ruled out (at the 3σ level) anywhere between 0.25 and 1AU. Similarly, over

the same region, our results imply that a uniform source of emission can not contribute more than 0.4% of excess in the near infrared. Clearly, if a hot debris disk is responsible for a substantial amount ($\geq 1\%$) of near infrared extra-emission, our observations indicate that it must either arise from within $\simeq 0.2\,\mathrm{AU}$, i.e in the close vicinity of the dust sublimation region, and/or from colder ($\leq 800\,\mathrm{K}$) regions located further away than $\simeq 1$ to $2\,\mathrm{AU}$. Further observational data are required to assess the viability of these two dust population scenarios and derive more physical information on the nature of a potential near infrared excess around Vega. This is the objective of the next section.

3. Comparison to existing high contrast high resolution data

3.1. NIR and MIR data

Here we review the existing data about the potential magnitude of an infrared excess within a few AU of Vega. Very few instruments have the required combination of spatial resolution and contrast to provide such information.

Very accurate near infrared observations of Vega have been obtained in K band with the FLUOR instrument of the CHARA long baseline interferometric array (Absil et al. 2006; Aufdenberg et al. 2006). In particular, these measurements show a "visibility deficit" at short baselines, which Absil et al. attribute to the probable presence of a hot debris disk, contributing about 1.3% of Vega's flux within the FLUOR field of view ($\simeq 7.8$ AU). In the mid infrared (at 10.6 μm), single telescope nulling observations have been conducted on the MMT using the BLINC instrument (Liu et al. 2004; Liu et al. 2009), concluding that there is no resolved emission from the circumstellar environment (at separations greater than 0.8 AU) above 2.1% (3 σ limit) of the level of the stellar photospheric emission. Additionally, the authors find that the null does not vary significantly with observations at different rotations of the interferometer baseline (over a range of about 90 degrees), indicating that there is no evidence of an inclined disk-like structure. Broad-band (8 to 13 μm) mid infrared measurements at higher spatial resolution were recently obtained by long baseline - separated aperture- nulling at the Keck Interferometer. In particular, measurements obtained as part of the instrument shared risk commissioning (June 2007, unpublished data), detected no significant excess either, with the excess leakage estimated to be 0.33% $\pm$ 0.25% at an effective wavelength of 9 μm.

Figure 4 summarizes the excess leakages measured with the PFN and CHARA instruments in the near infrared, and with the MMT and the Keck Interferometer Nuller (KIN) in the mid-infrared. The KIN results cover a small range in azimuth due to the fixed KI

baseline, while the CHARA, PFN and MMT results cover larger azimuth ranges: respectively 40, 60 and 95 degrees. To get a consistent view of the results provided by the different instruments, we converted the CHARA visibility deficit observed with their 34 m baseline into an equivalent excess leakage of $0.55\% \pm 0.1\%$. From the CHARA, MMT and KIN measured excess leakages, and using the simple ring model suggested above for the PFN data, we derive constraints on the relative flux of a putative geometrically and optically thin dust ring around Vega (Figure 5). As in the case of the PFN observations (section 3), this is done by folding in the sky transmission pattern for each of these 3 facilities. In the case of KIN, we use the transmission pattern computed at the time of the observations, including the effects of the short and long baseline fringes, together with the field of view limitations introduced by the camera optics (focal plane pinhole and finite spectral dispersion). Full details can be found in Colavita et al. 2009, as well as in Millan-Gabet et al. 2011 and Serabyn et al. 2011, both in preparation. For the MMT, we computed the expected sky transmission pattern from a 10.6 micron nuller formed of two 2.5 m sub-apertures separated by 4m. As in the case of the PFN, no excess was detected in the mid-infared by the KIN and MMT instruments, and the corresponding curves in Figure 5 represent the ring flux 3σ upper limits as a function of distance to the star. Also clearly apparent is the nice complementarity of the KIN and MMT mid-infrared data in terms of spatial scales covered.

For the CHARA (full K-band) data, we take into account the transmission pattern of a single-mode fiber optimized for coupling the light of a 1 m telescope (FWHM$\simeq 500$ mas), the interferometric fringe pattern (34 m baseline), and the coherence loss effects at the edge of the field. The dashed dotted curve of figure 5 shows the resulting excess flux detected - and its $\pm 1 \sigma$ boundaries - as a function of ring separation. The CHARA data alone hardly constrain the location of the excess within FLUOR's field of view. However, the constraints from the PFN (Figure 5) clearly show that any significant NIR excess (e.g. compatible with the CHARA data) must originate from within $\simeq 0.2$AU, and/or from further away than $\simeq 2$ AU. We now examine hereafter these two possibilities in more detail, assuming that Vega's brightness distribution did not change significantly between the May 2005 CHARA observations and the July 2009 PFN ones. Otherwise, no meaningful comparison can be made.

3.2. Interpretation

From the CHARA excess detection, and from Vega's tabulated flux, we can compute the corresponding absolute 2.2 μm flux of a narrow circumstellar ring, as a function of its distance to the star. Similarly, from the KIN and MMT upper limits, we calculate the (3

σ) upper limits to the absolute flux contributed by a dust ring around Vega (at 9 microns for KIN and at 10.6 microns for the MMT). From these NIR flux levels and from the MIR upper limits, we derive the "minimum" near to mid infrared ring flux ratio compatible with the data (plain curve, Figure 6 left). In comparison, the dashed curve shows the NIR/MIR flux ratio expected from dust emitting like a black-body at thermal equilibrium with the star, i.e. with a temperature radial profile going as $L^{0.25}/r^{0.5}$. For the stellar luminosity L, we use Vega's equatorial plane flux computed in Aufdenberg et al. 2006 (table 3), and find an equivalent luminosity of 28.9 L$\odot$. This value is smaller than Vega's observed - nearly pole-on - 37 L$\odot$ luminosity because of the large temperature gradient between the pole and the equator. For any realistic dust ring radius (i.e T < 2000K, and r≥ 0.1 AU), the minimum NIR/MIR flux ratio observed is found to be significantly larger than that derived from a simplistic black-body assumption, by a factor of 3 or more. Considering a dust temperature profile decreasing more slowly than in the black-body case, as observed for instance in the solar system zodiacal cloud by COBE/DIRBE (T(r) $\propto L^{\delta/2}/r^{\delta}$ with δ=0.467, (Kelsall et al. 1998)), the predicted flux ratio is even lower (Figure 6 left, dotted curve). Thus, relative to a single-temperature black body or grey body, either the MIR emission must be suppressed (by e.g., a low MIR emissivity), or the NIR emission must be strongly enhanced (e.g. by scattering) to be detected by CHARA.

3.2.1. Thermal emission

Detailed Mie calculations show that the emissivity of a spherical dust particle is roughly unity at wavelengths shorter that $2\pi a$, where a is the radius of the particle, falling off as λ^{-n}, with n $\simeq$ 1-2, at longer wavelengths. If the ring infrared brightness were dominated by thermal emission rather than scattering effects, Figure 6 (right) shows that beyond about 0.6 AU, the minimum NIR/MIR emissivity ratio required exceeds the value expected from a λ^{-2} emissivity law (the steepest emissivity decline predicted by Mie theory). The possibility of thermal emission from dust located further than 2AU is then ruled out. The CHARA observed excess would have to arise from a very narrow region, located between the sublimation radius (0.1 to 0.15 AU, given the uncertainties on grain properties and Vega's equatorial flux), and the 0.2AU upper limit set by the NIR PFN data. In addition, we find (Figure 6 left) that the NIR/MIR emissivity ratio must be greater than 3.5 everywhere between 0.1 and 0.2 AU to fit the data, and probably a few times higher since this is a 3σ lower limit . This implies dust grains significantly smaller than the MIR wavelength, i.e. micron sized or smaller.

This implication is quite different from the case of our own zodiacal disk, for which a

flat opacity spectrum until 150 microns implies a significant population of larger ($\simeq 10$ to 100 microns) grains (Fixsen & Dwek 2002). Any ring-like distribution of small grains around Vega would thus differ significantly from our own zodiacal disk in spatial distribution and grain size. collisions in a denser disk would be much more frequent. The small size of the grains is surprising, as radiation pressure is expected to expel small grains rapidly to tens or hundreds of AUs. One possibility is that the small grains are not expelled effectively by radiation pressure, a case that arises if the grains are predominantly very non-spherical or extremely small. This would for instance happen for grains similar in size to the nano (1-10 nm) dust particules trapped near the Sun and recently detected by the STEREO spacecraft (Mann et al. 2010). In this case the bright emission ring would be located near the sublimation radius, as we find. Another possibility is that small grains are continuously fed to the inner region because of dynamical perturbations and collisions in the outer colder disk of Vega, induced for instance by migrating planets. The resulting dust would then be transported inward by Poynting-Robertson drag and strong stellar winds, as recently suggested around ϵ Eri (Reidemeister et al. 2010). In a more speculative vein, abundant close-in small grains may on the other hand correspond to a bright turnaround region: as larger grains fall inward due to Poynting-Robertson drag, they encounter increasing collision rates, leading to decreasing grain sizes and increasing emission, until the grains become small enough for radiation pressure to dominate and expel them. Finally, the ring-like distribution may instead signify clearing or shepherding by nearby planets.

3.2.2. Starlight scattering

Conversely, if scattering strongly dominates over thermal emission at NIR wavelengths, and is much less efficient at MIR wavelengths, both the inner (< 0.2AU) and outer (> 2AU) dust populations are a priori compatible with the data. A complete simulation of dust properties is necessary to explore these two possibilities, and is carried out in a separate paper (Defrere et al. 2011, in preparation) modeling both interferometric and spectral data. However, from a first analysis based on astronomical silicates (Draine & Lee 1984), small grains - typically micron sized or smaller - seem again necessary to produce strong scattering efficiency enhancement in the NIR. Finally, we note that if starlight scattering was responsible for a significant ($> 1\%$) NIR excess emission, it would essentially have the same color as Vega, and may have well remained undetected before the spatially resolved high accuracy CHARA observations.

4. Conclusions

Using the Palomar Fiber Nuller and the null self calibration technique, we have demonstrated high contrast imaging capabilities within the diffraction limit at the Palomar Hale telescope. We presented the deepest stellar nulls measured to date in the NIR (0.0008 ± 0.0004), providing new constraints on exo-zodiacal emission in the inner few AU around Vega. In particular, our data show that, if present at all, any significant ($\geq 1\%$) source of extended NIR excess must either be confined very close to the dust sublimation radius (and arise in either scattering or thermal emission), and/or come from a colder grain population located beyond 2 AU (compatible with scattering only). The absence of a corresponding MIR excess implies that such a NIR excess would most likely come from very small grains, micron sized or smaller.

Accurate ground-based nulling measurements have so far been limited to the mid-infrared, where one takes advantage of the reduced turbulence and improved wavefront quality. Our Palomar results demonstrate that although shorter wavelengths have intrinsically higher phase fluctuations, high contrast interferometry is also possible in the near infrared, providing higher spatial resolution and much better sensitivity from the ground. With the new PALM-3000 extreme AO system (Bouchez et al. 2008) coming on-line at Palomar in 2011, simulations indicate that contrasts of the order of 10^{-4} to 10^{-3} should be readily accessible with our system on $m_K = 3$ to $m_K = 6$ stars, as close as $30\,\text{mas}$ from the central star (Mennesson et al. 2010; Serabyn et al. 2010).

As illustrated by our initial PFN measurements of Vega, single telescope observations at this contrast and spatial resolution allow new constraints on the amount and spatial structure of exo-zodiacal light around nearby main sequence A stars. Additionally, the fiber nuller and null self-calibration techniques can be extended to long baseline interferometers, - as long as fringe tracking and dispersion capabilities are available (Mennesson 2011, in preparation) -, so that 10^{-3} contrast or better should also be accessible at much higher spatial resolution. This opens up the possibility of extending the high contrast NIR exo-zodi survey to nearby FGK main sequence stars, where hot dust is expected at smaller separations. This is a very attractive prospect, as exo-zodiacal light structure is a powerful tracer of planetary system's formation history and current dynamical activity, and also an important design parameter for future direct imaging missions targeting exoplanets in the habitable zone. Indeed, clumpy and/or large exo-zodi levels will be a hindrance to all types of missions, whether relying on visible coronagraphy or MIR interferometry.

REFERENCES

Absil, O. et al. 2006b, A&A 452, 237

Absil, O. et al. 2008, A&A 487, 1041

Absil, O. et al. 2009, ApJ, 704, 150

Akeson, R. et al. 2009, ApJ 691, 1896

Aufdenberg, J.P. et al. 2006, ApJ 645, 664

Aumann, H.H. 1985, PASP, 97, 885

Backman, D.E. & Paresce, F. 1993, Conference Proceedings, Protostars and Planets III, p. 1253-1304

Beichman C. & Velusamy T. 1997, AAS meeting 191, 29, 1310

Bouchez, A. et al. 2008, 2008, SPIE Conf. Ser. 7015, ed. N. Hubin, C. Max, P. L. Wizinowich, 24

Colavita, M. M. et al. 2009, PASP, 121,1120

Defrere, D. et al. 2010, A&A, 509, 9

Di Folco, E. et al. 2007, A&A 475, 243

Draine, B.T. & Lee, H.M., 1984, ApJ 285, 89

Eisner, J. A. et al. 2009, ApJ, 698, L169

Fixsen, D.J. & Dwek, E. 2002, ApJ, 578, 1009

Haguenauer, P. & Serabyn, E. 2006, Applied Optics, 45, 2749

Hanot, C. et al. 2011, ApJ, accepted for publication

Hinz, P. et al. 1998, Nature, 395, 251

Holland, W.S. et al. 1998, Nature, 392, 788

Kelsall et al. 1998, ApJ 508, 44

Liu, M.C. et al., ApJ, 610, 125

Liu, M.C. et al., ApJ, 693, 1500

Mann, I. et al. 2010, Twelfth International Solar Wind Conference, AIP Conf. Proc. , Vol. 1216, 491

Malbet, F. et al. 2005A&A, 437,637

Martin, S. et al. 2008, in SPIE Conf. Ser. 7013, Optical and Infrared Interferometry, ed. M. Scholler, W.C. Danchi, F. Delplancke, 57

Mennesson B. & Mariotti J.M. 1997, Icarus, 128, 202

Mennesson, B. et al. 2006, in SPIE Conf. Ser. 6268, Advances in Stellar Interferometry, ed. J.D. Monnier, M. Scholler, W.C. Danchi, 95

Mennesson et al. 2010, in SPIE Conf. Ser. 7735, Ground-based and Airborne Instrumentation for Astronomy III, ed I. S. McLean, S. K. Ramsay, H. Takami, 35

Millan-Gabet, R. et al. 2006, ApJ 645, L77

Monnier, J. et al. 2005, ApJ 632, 689

Tannirkulam, A. et al. 2008, ApJ 677, L51

Peterson D.M. et al. 1999, Nature, 440, 896

Reidemeister M. et al. 2010, arXiv:1011.4882

Serabyn, E & Mennesson, B. 2006, in Direct Imaging of Exoplanets: Science & Techniques. Proceedings of the IAU Colloquium 200, Edited by C. Aime and F. Vakili, 379

Serabyn, E. et al 2010, in SPIE Conf. Ser. 7734, Optical and Infrared Interferometry II. Edited by W.C. Danchi, F. Delplancke, & J.K. Rajagopal, 41

Siegler, N. et al. 2007, ApJ 654, 580

Stock, N.D. et al. 2010, ApJ 724, 1238

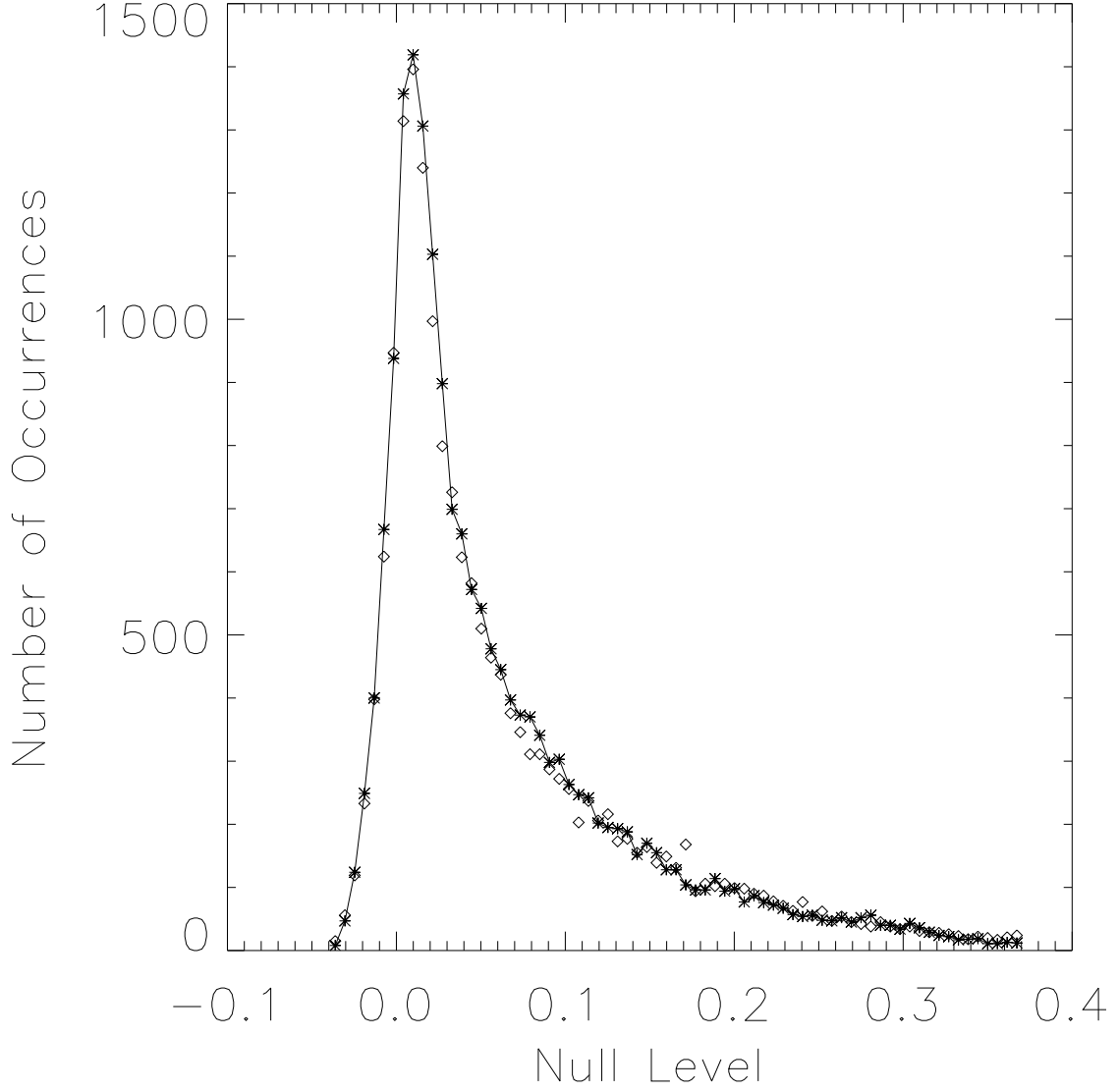Su, K.Y. L. et al. 2005, ApJ, 628, 487

Wilner, D. et al. 2002, ApJ, 569, 115

Fig. 1.— Distribution of null values recored on Vega with the Palomar Fiber Nuller for a baseline azimuth of 117°. Data points represented by asterisks show the observed number of occurrences in a given null interval, while diamonds indicate the values derived for the best fit model distribution. The underlying astrophysical null depth - close to the distribution peak- is found to be $N_a = 0.0012 \pm 0.0005$ (1σ) for the best fit model (reduced χ^2 of 1.15).
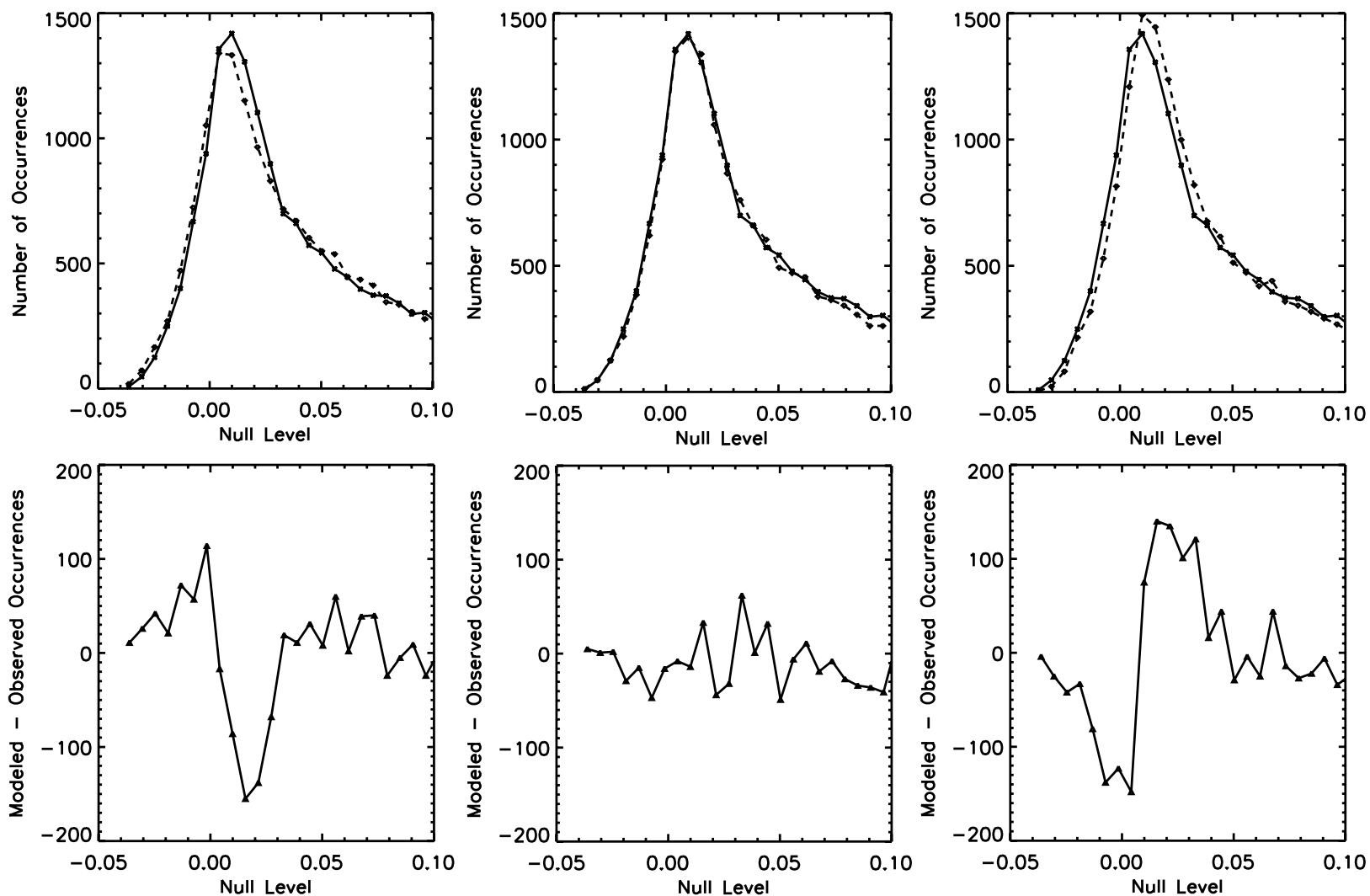
Fig. 2.— Different models of the null depth distribution measured on Vega (same data set as in Figure 1, but concentrating on the peak of the distribution). Asterisks show the observed number of occurrences in a given null interval, while diamonds indicate the values derived for a given model distribution. The underlying astrophysical null depth - close to the distribution peak- is found to be $N_a = 0.0012 \pm 0.0005$ (1σ) for the best fit model (reduced χ^2 of 1.15) represented in the center top panel. The top left and top right panels show the fits obtained when fixing the astrophysical null depth respectively -5σ and $+5$ σ away from the best fit value. The respective reduced χ^2 of these models are 2.57 and 3.09. The lower panels show residuals between the modeled and observed distributions for each of the three assumed astrophysical null values, illustrating the sensitivity of the method to null offsets as low as 0.0025.
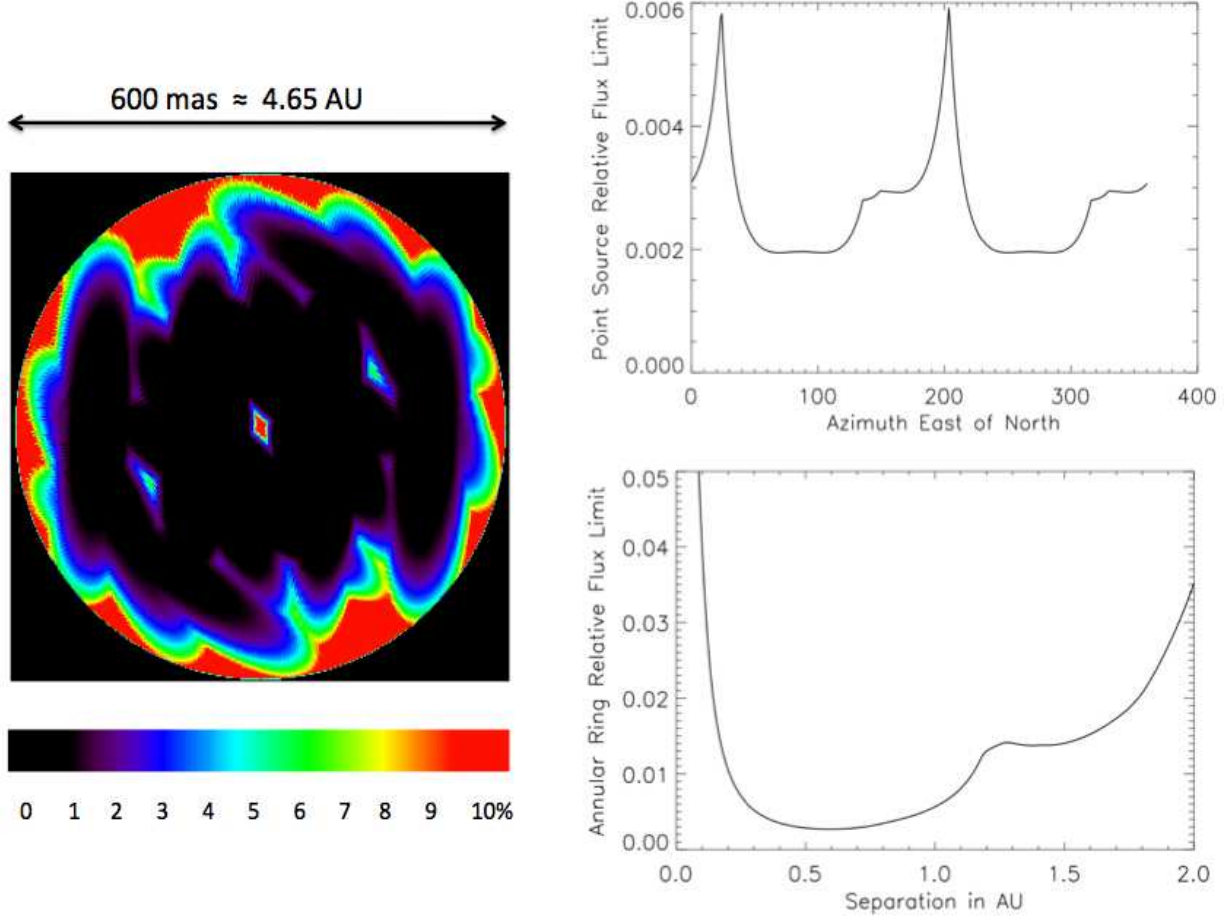
Fig. 3.— Vega circumstellar emission upper limits derived from PFN data recorded at three baseline orientations. Left: map of the maximum (3σ) point source levels (relative to Vega) consistent with the PFN data. North is up, East is to the left. Field of view radius is 300 mas around Vega ($\simeq 2.3$ AU). As expected, constraints on a putative companion get looser at the edge of the fiber field of view, and at the center of the field, where destructive interference occurs for all baseline orientations. Right, top: Upper limit at 0.6 AU ($= 47$mas) as a function of source position angle. Right, bottom: azimuthal average of left map. This corresponds to the 3σ upper flux limit for a geometrically thin ring around Vega. It is consistently below 0.6% between 0.2AU ($\simeq 25$mas) and 1.0 AU ($\simeq 130$mas), and as low as 0.3% around 0.6 AU.
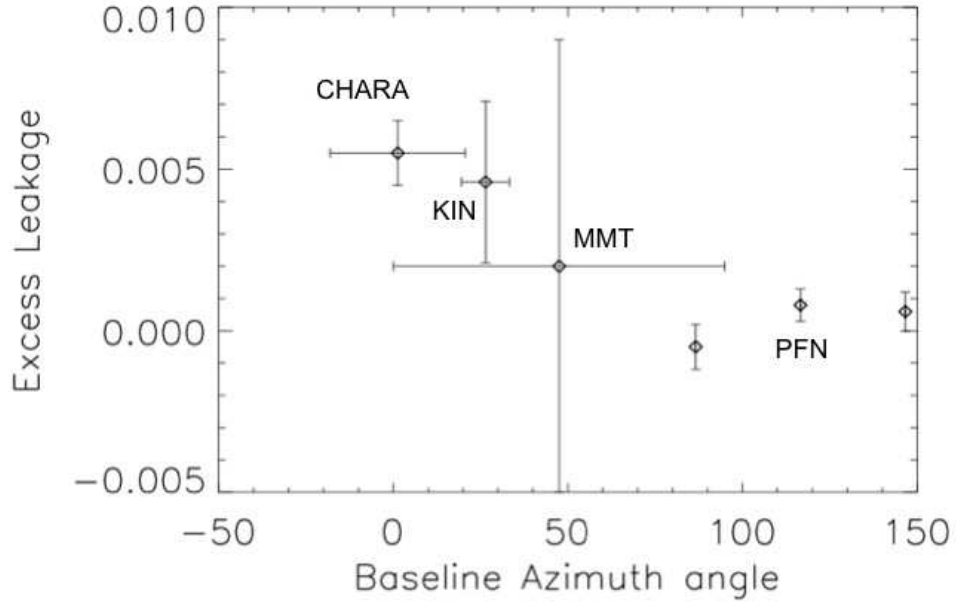
Fig. 4.— Excess leakage measured on Vega by various instruments at different baseline orientations (azimuth East of North in degrees). In all cases, the photospheric null has been subtracted and an excess leakage traces possible resolved sources of extra emission. CHARA data use a 34 m baseline at K band, and show a $> 5\sigma$ excess. In comparison, no significant excess is detected by the Palomar Fiber Nuller (PFN, baseline=3.4 m, also at K band), nor by the Keck Interferometer Nuller (KIN, baseline $= 85$ m, $\lambda \simeq 9$ μm) or the MMT (baseline $=4$ m, $\lambda \simeq 10.6$ μm).
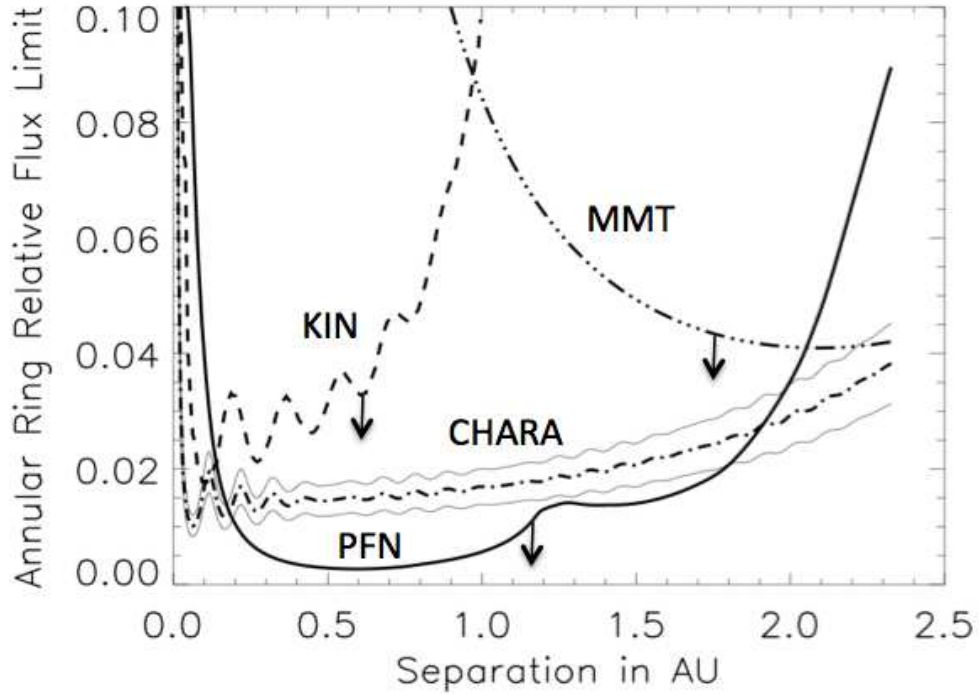
Fig. 5.— Flux constraints (relative to Vega) of a geometrically thin annular dust ring located at various stellocentric distances. The CHARA dash dotted curve (with its bracketing $\pm 1\sigma$ boundaries) is derived from the excess reported at K band (Absil et al. 2006). All other curves are upper limits (3σ) derived from the KIN (9 microns), MMT (10.6 microns) and PFN (K band) null measurements. Assuming no significant changes in the dust distribution between 2005 and 2009, the PFN data constrain the CHARA NIR excess to reside either within $\simeq 0.2$ AU and/or outside of $\simeq 2$AU of Vega.
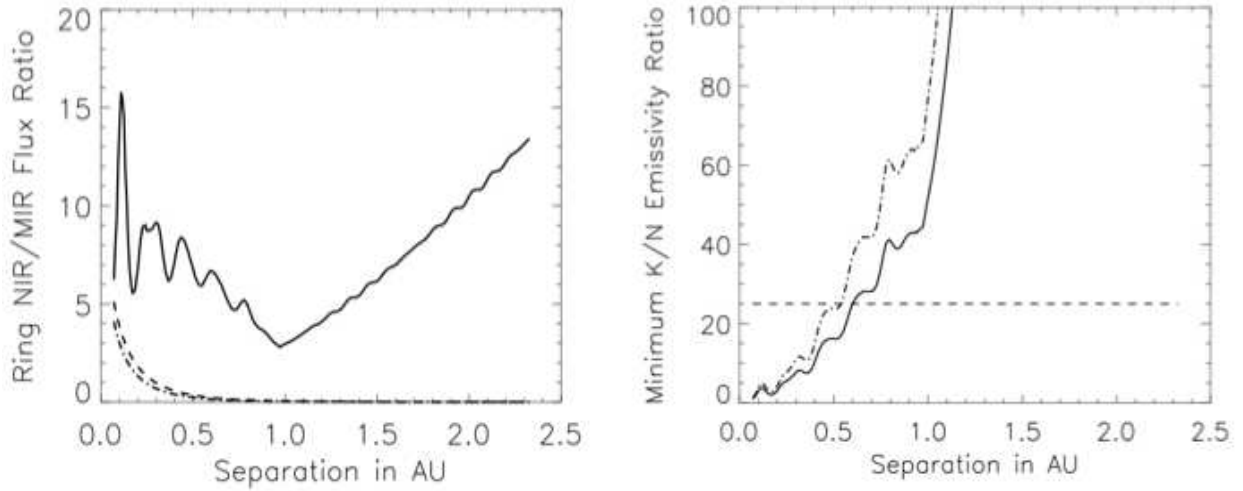
Fig. 6.— Left: near to mid infrared flux ratio of a geometrically thin dust ring located at various distances from Vega. Plain curve: minimum value consistent with the CHARA, KIN and MMT data. Dashed curve: value predicted for dust emitting as a black-body in thermal equilibrium with the star. Dash-dotted curve: value predicted for dust emitting as a grey body with a dust temperature profile analogous to the solar system case. The latter two curves assume for Vega an equatorial luminosity of 28.9 $L_\odot$. Right: Minimum near to mid infrared emissivity ratio compatible with the data, assuming pure thermal emission from a geometrically thin ring (plain curve: black-body model, dash-dotted curve: grey body model). For ring separations larger than $\simeq 0.6$ AU, the emissivity ratio takes values larger than predicted by a λ^{-2} power law (horizontal dashed line), pointing to a non thermal emission process.

Table 1. Summary of Vega PFN observations

Az (°)	N_a	σ	Residual Null	Excess 3σ Upper Limit
87	-1×10^{-4}	7×10^{-4}	-5×10^{-4}	1.6×10^{-3}
117	12×10^{-4}	5×10^{-4}	8×10^{-4}	2.3×10^{-3}
147	10×10^{-4}	6×10^{-4}	6×10^{-4}	2.4×10^{-3}

Note. — Az is the baseline azimuth measured in degrees East of North. N_a is the measured astrophysical null. The residual null (or "excess leakage") is computed by subtracting the null depth expected from Vega's photosphere, which is $4.0\ 10^{-4}$ at the PFN 3.20m baseline and 2.16 μm effective wavelength.